Task: Active Tropospheric Ozone and Moisture Sounder (ATOMS)
Trade Study Area: Tropospheric Studies

E. R. Kursinski (erk@cobra.jpl.nasa.gov)
George A. Hajj (george.a.hajj@jpl.nasa.gov)
Thomas P. Yunck (tpy@cobra.jpl.nasa.gov)
Jet Propulsion Laboratory, California Institute of Technology

Benjamin M. Herman (herman@air.atmo.arizona.edu)
University of Arizona, Institute of Atmospheric Physics

Final Report
February 16, 1999

1. Introduction

The success of the GPS atmospheric occultation technique, first performed on the GPS/MET flight experiment aboard NASA's MicroLab-1 spacecraft, has established the potential of active radio occultation sounding. The GPS/MET investigation has delivered precise temperature, pressure and density profiles between 4 and 40 km altitude using the 1.2 and 1.6 GHz GPS transmissions.

With additional frequencies in the 10-200 GHz range, the radio occultation method can be extended to allow retrievals of other species. In this study we have examined satellite-to-satellite occultation crosslink sensing in the 10-200 GHz range between pairs of low Earth orbiting (LEO) satellites. In a full implementation we envision a constellation of perhaps dozens of LEO microsats exchanging microwave crosslinks between all occulting pairs to produce many thousands of uniformly distributed atmospheric soundings each day. With the proper selection of frequencies, these soundings will produce precise profiles of tropospheric and stratospheric ozone (at ~110 GHz) and water vapor (at ~22 and 183 GHz) with better than 1 km vertical resolution. At present there are no satisfactory means of acquiring synoptic ozone and water vapor measurements throughout the troposphere, yet ozone and water vapor are two of the most critical and sought-after components of and contributors to Earth's changing atmospheric chemistry and climate. A rigorous understanding of their concentration and evolution at all levels of the atmosphere is a vital concern of current Earth system science research.

A constellation of 32 microsats distributed uniformly in two nested constellations of 16 satellites each, at altitudes of 700 and 850 km and inclinations of 65-75 degrees, will deliver about 11,000 atmospheric crosslink occultation profiles each day. However, in contrast to microwave technology at 30 GHz and below, which is quite mature, instrumentation for active transmission above 60 GHz is rather primitive and largely unexamined as a means of Earth remote sensing.

The principal objective of the ATOMS Trade Study was to perform simulation studies of the crosslink occultation technique over frequencies from 10 to 200 GHz to assess its potential performance and feasibility as a method of sensing tropospheric moisture and ozone. A second objective was to assess the state of current microwave hardware in the desired frequency range. The studies were carried out in as collaboration between JPL and the Institute of Atmospheric Physics at the University of Arizona.

2. Determining Global Coverage

In a preliminary study computer simulations were conducted to determine the global coverage to be achieved with crosslink radio occultations for constellations of 8, 12, 32, and 50 LEO satellites. These produced, respectively, 800, 1600, 11,000, and 25,000 globally distributed occultations.

The coverage achievable with a 32-satellite constellation is shown in Fig. 1. These studies were done simply to get an idea of the numbers of instruments that would have to be deployed for adequate coverage, to understand whether this approach can reasonably produce the required number of measurements and is thus worth pursuing further. These results show that outstanding coverage can be achieved with a relatively small number of sensors.

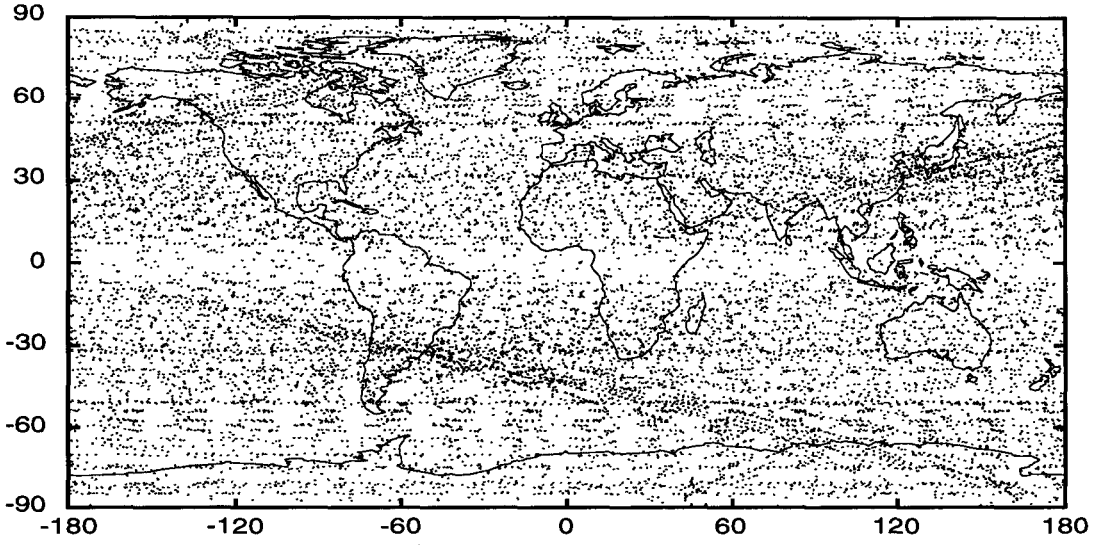

Fig. 1. A 32-satellite LEO constellation will provide over 11,000 daily crosslink occultations. Further optimization of the constellation will give improved uniformity of sampling.

3. Preliminary Study of Water Vapor Profiling

Water vapor absorbs strongly at 183 GHz and 22.2 GHz and less strongly at frequencies in between and below, down to about 10 GHz. Changes in measured amplitude at several selected frequencies can thus directly reveal water vapor concentration and distribution. The amplitude measurements reveal the total extinction along the ray path. The unattenuated signal above the atmosphere, before or after the occultation, is used to calibrate the absolute signal level. The attenuation through the atmosphere gives a direct measure of the amount of attenuating matter. In the upper troposphere, where moisture is rare, we employ the strongly absorbed 183 and 22 GHz signals along with one or two nearby frequencies to cancel the effects of continuum absorption. In the lower troposphere where moisture is abundant we switch to the 10-17 GHz signals.

By using the full 10-200 GHz frequency range we expect to measure H_2O profiles from the lower stratosphere to near the surface under most conditions. These measurements should be accurate to a few ppm at the tropopause, degrading to about 5% in the lower few kilometers where water vapor is abundant. Figure 2 shows a typical water vapor retrieval simulation generated by our team at the Univ. of Arizona. The simulations incorporated ±2 K random temperature errors and ±1% random measurement errors. Figure 3 shows the vertical distribution of the retrieval errors. While the simulations omit several other key errors, including diffraction, defocusing, and absorption by other atmospheric constituents, they serve to illustrate the technique's potential. Additional errors will be included in later simulations to obtain a more realistic estimate of the achievable measurement accuracy.

4. Preliminary Survey of Available Hardware

A principal technical question is whether we can generate suitable crosslink signals in the first place. A very preliminary investigations reveals that electronics for above-100 GHz transmission

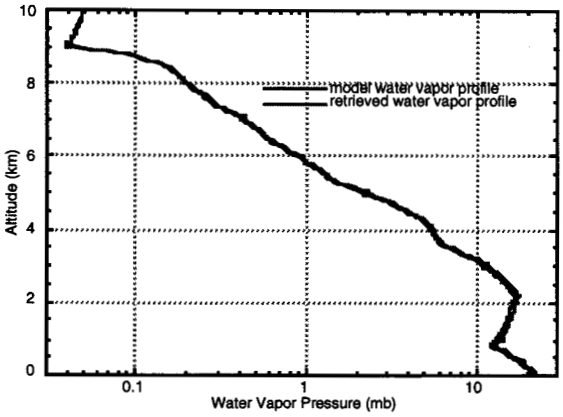

Fig. 2. Simulated tropical water vapor profile modified to include irregularities, and the retrieved profile. Retrieval is shown only to 10 km.

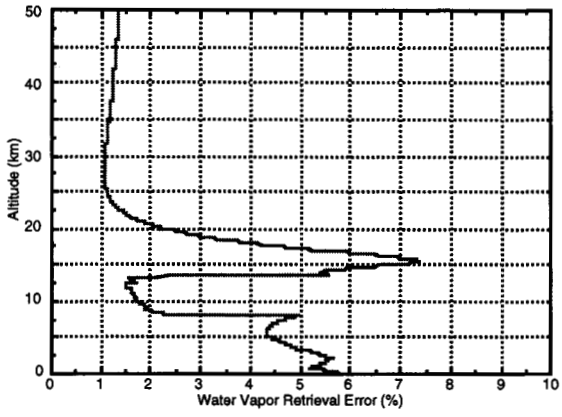

Fig. 3. Percent errors in the simulated water vapor profile retrieval shown at left.

are at present fairly primitive and inefficient, delivering radiated power less than 10% of the input power. Such systems as are available can generally achieve less than 1 W of sustained transmitted power. The effective radiated power can be readily increased with suitably high antenna gain (compressing the signal into a narrower beam with a dish or phased array antenna), but this then leads to more exacting pointing constraints. This initial survey has only scratched the surface; much more must be done in the next two months to understand the state of current crosslink technology.

5. Study of Ozone Sounding at 110 and 165 GHz

Ozone has absorption lines at 101, 110 and 165 GHz, enabling its presence to be detected with active radio occultation. The recovery and error correction methods are essentially the same as outlined in the last report for water vapor, slightly retuned for these frequencies. Figure 4 shows the transmission of a signal through the atmospheric limb at 110 and 165 GHz as a function of tangent height. Part of the extinction is due to O3 and part due to background O2 and H2O continuum absorption. Because this continuum background is essentially constant over the width of the O3 line, it may be easily removed by taking the ratio of the signal at two wavelengths within the O3 line, or by independent temperature vs pressure profiles determined from phase measurements using the same techniques employed for GPS/MET.

Excessive continuum absorption in the lower troposphere (below about 8 km) will define the lower altitude limit for the ozone profile. ATOMS will employ a frequency pair with one frequency at or near the line center and the second off center. The preferred frequencies will be determined during the first year studies. Figure 5 shows a simulated O_3 retrieval using a 165 GHz signal only. Errors of ±1 K were put into the temperature observations, ±0.1% into the calculated relative intensity observations, ±1% into pressure, and ±5% into the water vapor pressure. The retrieval and model agree to within ±1% above about 10 km, and within ±10% between 8.5-10 km. Figure 6 shows the vertical distribution of retrieval errors, with rapid degradation below 8 km.

We stress that we as yet lack clear evidence that all potential error sources can be controlled at the needed levels, though this early analysis is promising. A central objective of this study is to examine key errors and calibration strategies to establish more firmly the limitations of the technique and realistically assess its promise as an atmospheric sensor.

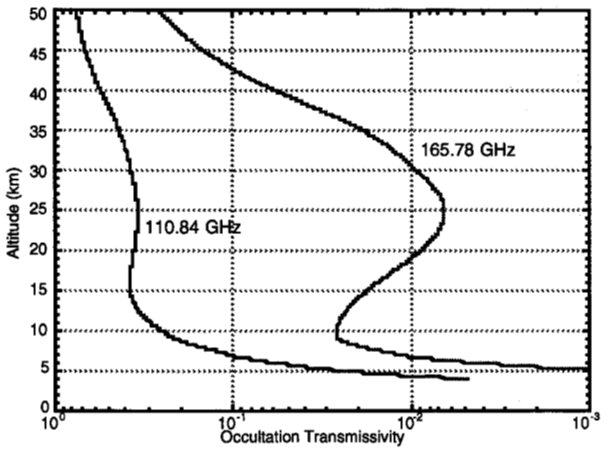

Fig. 4. Atmospheric transmissivities at the 165 and 110 GHz ozone lines. The "Modtran" standard atmospheric ozone distribution was used.

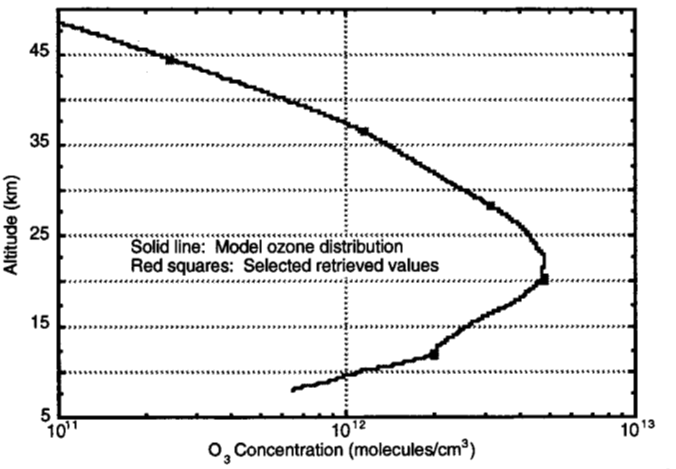

Fig. 5. Simulated ozone retrieval. Solid line is original distribution from the "Modtran" atmospheric model. Squares are retrieved values.

6. Detailed Studies at 10-23 GHz

In the limited time available for these studies we elected to focus on the most promising and most immediately realizable of the crosslink occultation techniques: tropospheric moisture sensing with frequencies between 10 and 23 GHz. The subsections that follow present the results of that study in some detail.

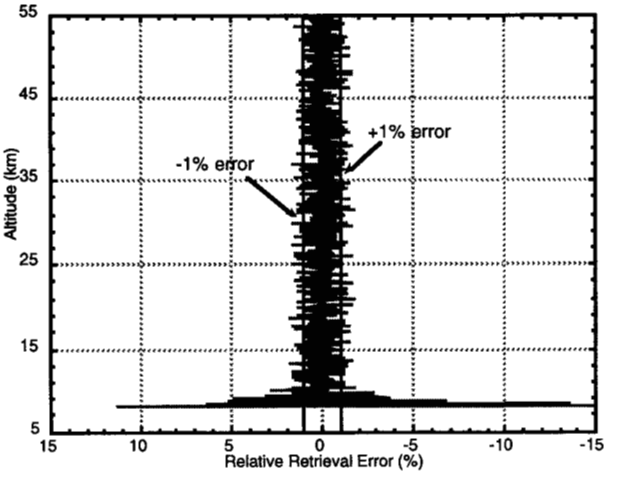

Fig. 6. Percentage errors in the retrieved ozone profile shown in Fig. 5.

6.1 Measurement Objectives

Water vapor in the upper troposphere at low latitudes: Water vapor mixing ratios near the tropical tropopause are very small (~3 ppm). Yet small amounts of water vapor in the upper troposphere exert a tremendous influence on the surface temperatures through radiative forcing, yet the amount and the mechanisms controlling water in the upper troposphere are uncertain. Discerning their influence requires their concentrations to be observed under different spatial, seasonal and diurnal conditions to expose the control mechanisms from which to infer how they may change in the future. Water vapor sensing in the upper troposphere at low latitudes requires both high sensitivity because of the low mixing ratios and vertical resolution of 1 km or better, consistent with the small water vapor scale height at altitude.

The sensitivity goal in the upper troposphere after averaging several profiles is 1 ppm and better with <1 km vertical resolution, which would allow observation of tropical tropopause mixing ratios of ~3 ppm and all levels below. Individual profile accuracy will be ~5 ppm with 1 km vertical resolution. Regional averaging of 25 profiles will yield ~ 1 ppm accuracy.

Middle and lower troposphere water vapor: For mixing ratios of 300 ppm or greater, water vapor profiles will be accurate to ~2% in clear and ~10% or better in cloudy conditions with a vertical resolution of 1 km or better.

Liquid water clouds: Liquid water cloud profiles and possibly profiles of rain will be derived in the lower troposphere via their frequency dependent absorption signatures.

Tropospheric temperature and geopotential: Accuracies of individual temperature and geopotential profiles will be $\leq$ 0. 3 - 2 K and 10-20 m accuracy through most of the troposphere. Accuracies of climatological averages will be 0.01 to 0.1 K and < 1 m for temperature and geopotential respectively.

Stratospheric and mesospheric temperature and geopotential: As noted above, crosslink temperature and geopotential profiles will extend much higher than the GNSS profiles, and individual profiles will achieve <1K temperature accuracy with 1 km or better vertical resolution up to at least 70 km. The accuracy of climatological averages derived from these profiles will be at least an order of magnitude better.

6.2 Retrieval Approach

The key steps in the crosslink occultation retrieval process are:

1. Measure the amplitude and phase of occulted signals at four frequencies from 10 to 23 GHz.
2. Remove variations in signal amplitude due to instrumental effects.
3. Derive a high resolution refractivity profile
4. Remove the variations in signal amplitude due to non-absorption atmospheric effects.
5. Smooth limb-path absorption estimates to ~1 km resolution.
6. Convert limb-path absorption profiles to radial profiles of absorption coefficient.
7. Combine the absorption profiles at multiple frequencies with the refractivity profile to derive profiles of water vapor, temperature, pressure, and cloud liquid and possibly rain.
8. Derive spatial and temporal averages.

We have three options for processing the data to derive water vapor, liquid water, temperature and pressure profiles. In all cases, the instrumental effects are first removed from the observations. The signals are then back-propagated from the point of reception through the vacuum to a reception point closer to the Earth's limb. This is possible because the signals are monochromatic with well-defined phase and amplitude. This approach has been known since the mid-1980's when it was used to dramatically improve the resolution of Saturn ring occultation data. The approach has been developed and used in atmospheric applications. Backpropagation both improves the diffraction limited resolution to ~25 m based on experiments with GPS data and removes atmospheric multipath, the effect where signal paths cross before reaching the receiver.

The key to sensitivity in the upper troposphere lies principally in how the non-absorption atmospheric effects are removed. The first scheme is designed to retrieve water vapor, temperature and pressure profiles in the upper and middle atmosphere where it is too cold in general for water to exist in the liquid state. The second scheme is designed to retrieve water vapor, temperature, pressure and liquid water profiles in the lower troposphere when liquid-water clouds are present. In each of these schemes, the effects of defocusing and diffraction are removed by ratioing the measured intensity at 22.6 GHz with that observed at 18 GHz, then smoothing the resulting ratio to 1 km resolution. In scheme 3 the effects of defocusing and diffraction are estimated by numerically forward propagating signals through the atmosphere described by the high resolution refractivity structure. The ratio of the observed signal intensity to the forward propagation estimate is then formed to isolate the effects of absorption. This ratio is then smoothed to ~1 km to reduce residual diffraction effects.

Residual amplitude variations due to diffraction associated with sharp structures and inhomogeneities will be on scales of ~25 m and will therefore average down rapidly when smoothed to ~1 km resolution. Noise associated with the finite SNR will average down by sqrt(n).

To obtain a retrieval we must convert absorption intensities into profiles of absorption coefficients. The signal level due to opacity is $I_0 e^{-\tau}$ where I_0 is the intensity in the absence of the atmosphere and τ is the optical depth. For each wavelength, the optical depth, τ, is estimated as the natural logarithm of the ratio of the absorption intensity to the vacuum intensity, (signal intensity with no atmosphere). We pass the profile of τ through an opacity Abel transform to derive a profile of the absorption coefficient at each wavelength. The opacity-extinction coefficient transform pair is given as

$$\tau = \int k d\ell = 2\int_{r_0}^{\infty} k \frac{nrdr}{\left(n^2 r^2 - n_0^2 r_0^2\right)^{1/2}} \quad <=> \quad k = -\frac{1}{2\pi}\frac{da}{dr}\bigg|_{a=a_0} \int_{a_0}^{\infty} \frac{d\tau}{da}\frac{da}{\left(a^2 - a_0^2\right)^{1/2}}$$

where k is the extinction coefficient. The four absorption coefficient profiles corresponding to the 10, 14, 18 and 22.6 GHz crosslink signals, and the refractivity profile are used to derive profiles of water vapor, temperature, pressure, cloud liquid and possibly rain rate. This is accomplished by use of the frequency dependent functional form of absorption of oxygen, water vapor, cloud liquid water and rain rate, along with the equations of refractivity, state and hydrostatic equilibrium. Multiple profiles are then binned and averaged over regions and monthly time scales for climate research.

Since we are using coherent signals to measure their intensity reduction due to absorption, the relationship between amplitude and intensity errors must be considered. Since intensity is proportional to amplitude squared, the intensity error is related to errors in amplitude by

$$\frac{\varepsilon_I}{I} = 2\frac{\varepsilon_A}{A} + \frac{\varepsilon_A^2}{A^2} \qquad (1)$$

where I is the intensity, A is amplitude and ε is the error. On short integration time scales of relevance to the occultation profiles the fractional amplitude error term (1st term on RHS of (1)) dominates. This term may have a zero mean and contributes little to climatological averages. Term 2 on the RHS of (1) is a bias because it is always positive. However, it can be made very small. Because of the factor of 2 in (1), fractional amplitude errors must be held to no more than one half the required intensity error.

A goal of 3 ppm in the upper troposphere implies sensitivity to changes in I of 0.23% and errors in A of less than 0.12%. The instrument will then be able to derive water vapor in the middle and lower troposphere with accuracies of ~2% or better in clear air. Furthermore, the high SNR's required will enhance the ability to penetrate liquid water clouds and rain. The critical portion of each occultation for deriving upper tropospheric water vapor is the ~15 sec over which the occulted signal tangent point descends from the stratopause (50 km), where there is virtually no defocusing, to the mid-troposphere (~8 km). A crucial requirement is therefore to hold uncertainties in the amplitude variations to < 0.1 % over this 15-sec interval. An error budget for measuring upper tropospheric water vapor is given in Table 1.

Table 1. Error budget for crosslinks in the upper troposphere

Error Source	Intensity error (%)
Transmitter (2)	0.1
Receiver (2)	0.1
Trans. Antenna	0.02
Receive Antenna	0.02
Voltage SNR = 3400 (2)	0.13
Local MP (2)	0.1
Intensity ratioing	0.25
Oxygen absorption (2)	0.02
Root Sum of Squares	0.39
Equivalent Sensitivity to WV	4.5 ppm

6.3 Instrumental Error Sources

Transmitter power: Since the transmitter power will vary, particularly after it is turned on, a power sensor will measure the output of each transmitter to an accuracy of 0.1% or better.

Antenna pointing: The antenna gain required to achieved a 1-sec SNR_v of 3400 is 28.5 dBi. At 22 GHz the gain of such an antenna is down by 0.1% relative to maximum at ~0.1 degrees off boresight. The spacecraft will therefore control pointing to 0.1 deg and provide pointing knowledge of 0.01 deg intensity variation due to antenna pointing uncertainty will be <0.02%.

Receiver gain: Since the LNA is common to the two received frequencies (see crosslink block diagram), gain variations in the LNA will be canceled when the ratio of the two frequencies is formed. Since gain varies by 0.1 dB per °C, the receiver temperature changes will kept <0.04 C (corresponding to intensity change of 0.1%) over any 15-sec interval. The temperature control will be accomplished passively through thermal isolation and inertia. In addition temperature changes along the receiver stages will be measured to $\leq$ 0.04 C.

Local multipath: Maintaining intensity variations due to local multipath to $\leq$ 0.1% requires that multipath signals be 66 dBc. A horn antenna will reject local multipath to at least 60 dBc based on results for the GRACE antenna. The additional 6 dB can be achieved with absorbing material on the spacecraft underside.

Phase stability: Phase jitter over the amplitude estimation interval will affect the amplitude error. There will be a bias due to term 2 on the RHS of (1). To control this we will estimate amplitude every msec and average the amplitude estimates over the ~0.3 sec associated with 1 km resolution. The phase stability required over 1 millisecond is 10^{-10}, which is easily achieved with a good crystal oscillator.

6.4 Non-absorption Atmospheric Effects

Removal of non-absorption effects in the atmosphere is crucial. These effects include defocusing from differential ray bending and diffraction by sharp inhomogeneities in refractivity. A smaller effect is associated with focusing due to the curvature of the Earth in the cross-track direction. The defocusing and diffraction effects must be considered together. Defocusing is independent of frequency whereas diffraction effects scale as $f^{1/2}$.

Accuracy of intensity ratioing in approaches 1 and 2: In these schemes, the ratios of the amplitudes of adjacent frequencies are formed and smoothed to the desired resolution. This works well when the frequencies are sufficiently close that diffraction effects largely cancel and when wavelengths are sufficiently small that the Fresnel scale is small in comparison to the desired resolution. Under these conditions, when the intensity ratio results are smoothed, the residual diffraction pattern averages down rapidly. Our occultation diffraction simulations used high resolution radiosonde data to define the refractivity. When the 22.6 and 18 GHz signals are ratioed and smoothed to 1 km resolution the rms of the residual intensity error is <0.25%, equivalent to a water vapor sensitivity of 5 ppm in the upper troposphere.

Accuracy of forward propagator: Simulations indicate the accuracy of the forward propagation ratio approach (scheme 3) is comparable to or surpasses the other two. With improvements in the forward propagator it may provide better results because it better accounts for the effects of diffraction. It also provides a degree of independence for cross-checking the retrieval results which we will use in the validation phase as well as an assessment of how well we understand the physics of observations.

The accuracy of the simulated phase and amplitude from the forward propagator depends on the quality of the refractivity profile which in turn depends on the quality of the occultation phase. Phase errors due to the SNR, reference oscillator, and ionosphere will all produce errors in the refractivity profile of 10^{-4} N-units or less. This will produce errors of 0.02% or less in the forward modeling of diffraction and defocusing when smoothed to 1 km resolution.

Based on simulations and parameters variation in the forward propagator, the standard deviation of errors in forward propagation is ~3%. These are errors in the very fine scale diffraction pattern and therefore have high Fourier frequencies and average down significantly when the results are vertically smoothed to ~1 km. Simulations indicate the standard deviation of errors in the 1 km smoothed estimates are reduced to ~0.2%. Biases in the forward propagator are less than 0.1%.

Amplitude Scintillations: When scintillations are weak, phase and amplitude effects are related in such a way that they can be treated similarly to diffraction from edges. Therefore the ratioing of the intensities at two frequencies will reduce the diffraction from the scintillations in much the way it does for edge diffraction. GPS/MET results show there is little if any evidence of scintillations in the upper troposphere, implying amplitude scintillations must be 0.1% or smaller. Scintillations at 22.6 GHz could thus be as large as 1%, weak enough that ratioing of the 22.6 and 18 GHz signal intensities and smoothing should attenuate the effect to less than 0.1%.

Scintillations in the lower troposphere will be larger. Since scintillation magnitude is roughly proportional to frequency, it can be limited by selecting a low frequency. Thompson et al. (1975) measured scintillations at five frequencies between 10 and 33 GHz over a 64 km path length between Haleakala, Maui and Upolu Point, Hawaii. Based on these data and an approximately linear scaling of weak amplitude scintillation magnitude with increased path length, the 10 and 14 GHz signals should seldom experience strong scintillations even under the very moist conditions of a subtropical boundary layer.

Focusing in the cross-track direction: Due to the Earth's curvature there is slight focusing in the cross track direction. Focusing in the upper troposphere is ~0.1%, while the maximum value near the surface can approach 1%. The bending angle estimates derived from the phase measurements will be extremely accurate, and the cross-track focusing term can be calibrated to a negligible level. The crosstrack focusing will also be eliminated by ratioing the amplitudes at two different frequencies.

Molecular oxygen: O_2 is the other major gaseous absorber at 10 to 23 GHz. At 17 km, absorption by O_2 at 22 GHz is ~15 times greater than by water vapor. Since O_2 is well mixed, we can use

the refractivity, which provides an estimate of the gas density to ~0.2% accuracy in the upper troposphere (Kursinski et al., 1997). This allows us to estimate and remove the oxygen absorption effect. Any uncertainty in the functional form of the oxygen absorption line will effectively cancel as we ratio the 22.6 and 18 GHz signals.

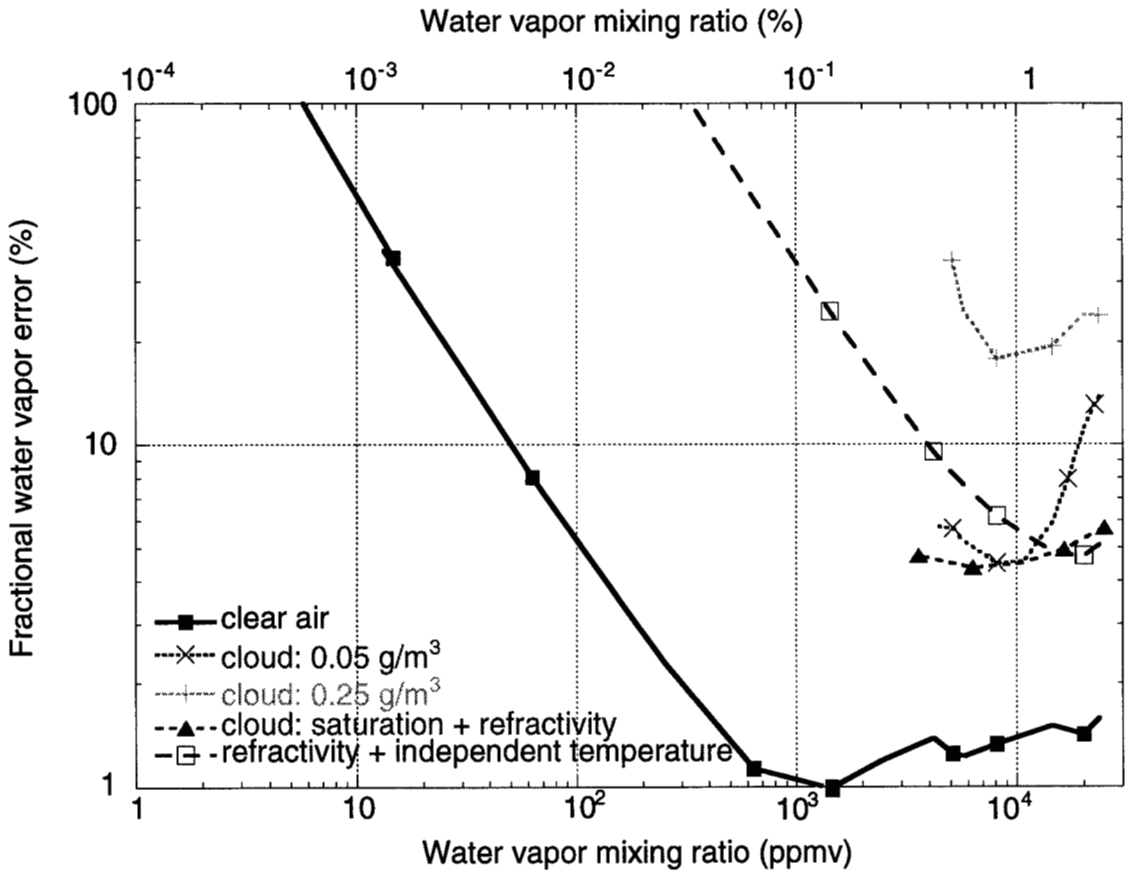

Fig. 7. *Crosslink water vapor profile accuracy vs mixing ratio.*

6.5 Clear Sky Accuracy

Absorption by liquid water will be determined from the frequency dependence of the observed attenuation. In the absence of liquid water, the absorption (after removal of molecular oxygen absorption) will be due only to vapor, and the vapor concentration will be determined by optimally weighting the four absorption estimates. The clear air results shown in Fig. 7 reflect the basic behavior. At small mixing ratios, the opacity of the water line is small and the mixing ratio error is approximately constant. The fractional error decreases linearly as the concentration grows, until the optical depth reaches 1. At still higher mixing ratios and opacities, the mixing ratio error increases more rapidly than the mixing ratio itself and the fractional accuracy decreases. The bump near a mixing ratio of 0.4% represents the transition between the 22.6 and 18 GHz as the primary source of information, where the 22.6 opacity grows beyond 1 while the 18 GHz opacity approaches 1. The relatively flat behavior at higher mixing ratios reflects an optimal use of the 18, 14 and 10 GHz signal intensities. These results include the effects of defocusing and assume the transmitters emit equal at all four frequencies power while the gain of the antenna scales as f^2.

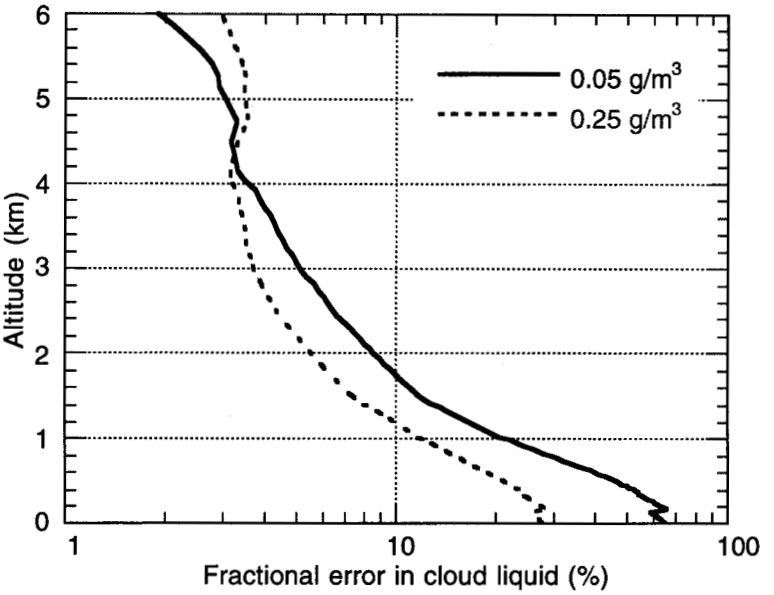

Fig. 8. *Crosslink water vapor profile accuracy vs mixing ratio.*

6.6 Water Vapor Accuracy in Presence of Clouds

Ice absorption and scattering at the crosslink wavelengths are so small that the accuracy in the presence of ice clouds will be the same as in clear sky. When the frequency dependent absorption signature of liquid water appears in the profiles, multiple signals must be used in combination to estimate both vapor and cloud liquid concentrations. This reduces the water vapor accuracy relative to clear air conditions because of correlation between the frequency dependence of the vapor and liquid absorption as well as a further increase in opacity.

When the clouds extend along all or most of the occultation path, such as marine stratus, the near-saturation condition of air along the path provides an additional constraint which allows separation of the water vapor and temperature contributions to refractivity. For sufficiently opaque clouds, this estimate becomes better than the direct separation of vapor and liquid.

Another approach when highly opaque clouds are present is to combine refractivity with independent temperature estimates, as we do with GNSS occultations. This approach can also be more accurate than direct separation of the liquid and vapor contributions under high opacity cloud conditions. Thus even in thick water clouds the water vapor accuracy will be 10% or better.

6.7 Liquid Water Cloud Profile Accuracy

The crosslinks can also sense liquid water in clouds, particularly stratus clouds. After defocusing in the lower troposphere and the residual error after calibration of defocusing and diffraction, cloud accuracies are $\leq$ 30% for much of the 0.05 to 0.25 g/m^3 range of cloud liquid water (Fig. 8).

If cloud is distributed along only part of the path, opacities will be smaller and direct separation of water vapor and liquid will be more accurate for a given cloud liquid concentration without assuming saturation. However, the partial distribution along the path will cause some errors in the intensity Abel transform which assumes opacity is a function of radius only. Use of weather satellite imagery will help determine the cloud distribution along the path. With this information we can generalize the intensity Abel transform.

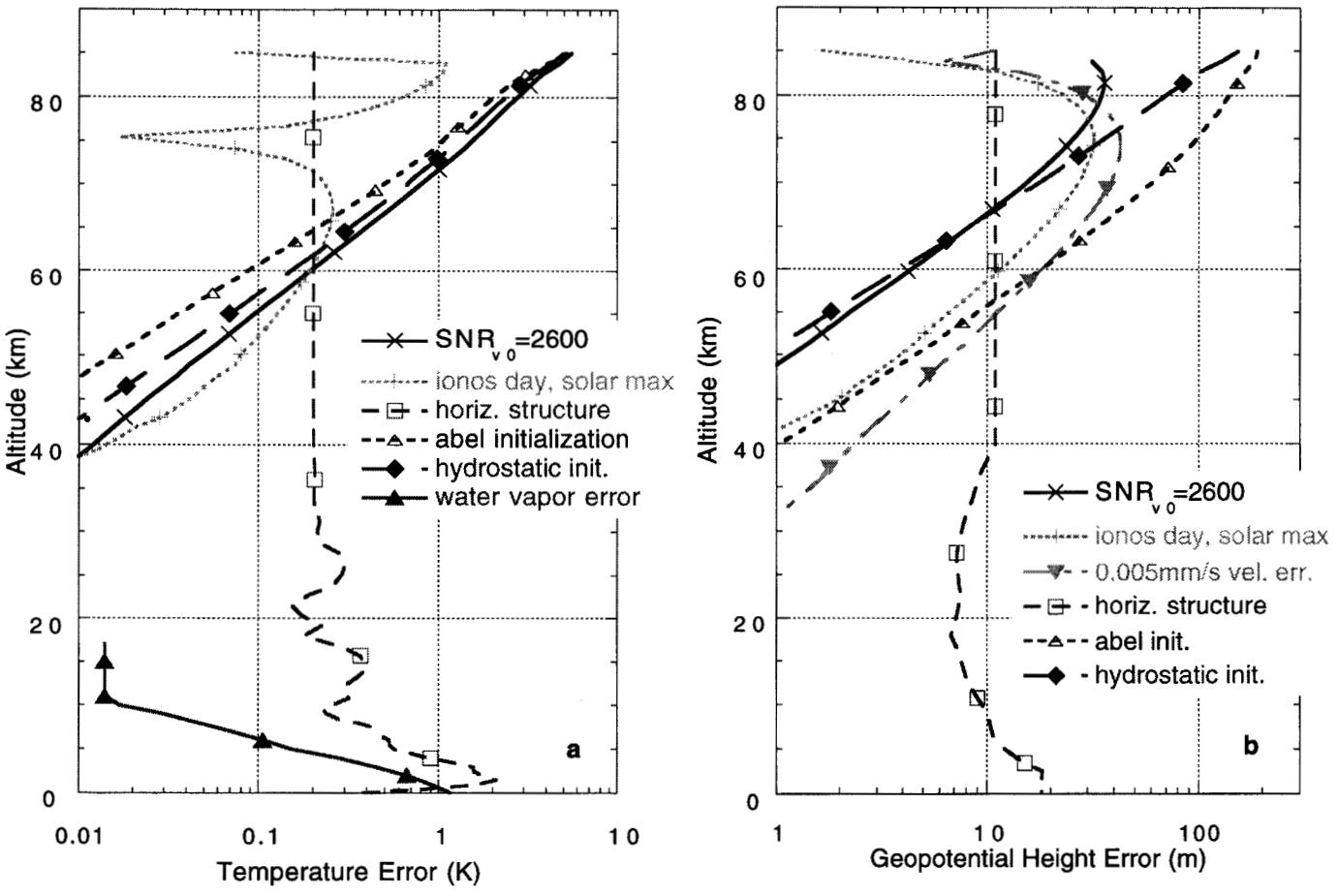

Fig. 9. *Predicted accuracy of Temperature and Geopotential Height Profiles with 10-23 GHz Crosslinks*

6.8 Temperature & Pressure-Geopotential Accuracy

In the middle atmosphere, crosslink occultation accuracies and altitude range will far surpass those of the GNSS occultations. Ionospheric refractivity at 22.7 GHz will be smaller than at GNSS wavelengths by a factor of ~ 200. The effects of phase jitter due to the finite SNR will be smaller than those at GNSS frequencies by a factor of ~60. Local multipath will be reduced by more than two orders of magnitude by the directional crosslink antennas. Orbital velocity errors will be reduced by an order of magnitude or more by extending the crosslink observation for 10 sec above the detectable atmosphere. As a result, the altitude range over which profile accuracies will be better than 1 K extends from the lower troposphere to ~70 km (Fig. 9a). Geopotential height errors of pressure profiles will be below 10 m from 10 to 23 km, and below 7-20 m from the surface to 60 km (Fig. 9b). Climatological averages will be at least an order of magnitude more accurate than the individual profiles, with accuracies of 0.03 K or better and ~1 m or better in geopotential height of pressure surfaces through most of the troposphere, stratosphere and mesosphere.

7. Conclusions and Future Directions

These studies demonstrate the considerable promise of the crosslink occultation technique for both ozone and moisture sensing throughout the troposphere. In the limited time available we could focus on only a few key issues: preliminary simulations of ozone and moisture sensing with signals above 100 GHz, and more in-depth simulations for moisture sensing with the more mature technology at 10-23 GHz. The technique at the lower frequencies is particularly promising, the hardware is mature, and (by a quick survey not described here) there appear to be sufficient available spectral bands. A demonstration moisture sensor operating within the 10-23 GHz band could readily be built and flown within the next 3 years. Prospects at the higher frequencies are less certain and will require far more in-depth study. Indeed, the studies begun here will be continued under the ATOMS task within NASA's Instrument Incubator Program, beginning in March 1999. Key issues to be examined include:

1. A comprehensive survey of available technology at the higher frequencies

2. An evaluation of spectrum availability for tropospheric sounding

3. In-depth performance simulations over the range of frequencies from 10 to 200 GHz and selection of the optimum number and placement of frequencies

4. Design trades for prototype instruments

8. References

Kursinski, E. R., G. A. Hajj, J. T. Schofield, R. P. Linfield and K. R. Hardy, 1997, Observing Earth's atmosphere with radio occultation measurements using the Global Positioning System, *J. Geophys. Res.*, 102, 23429-23465.

Thompson, M. C., L. E. Wood, H. B. Janes and D. Smith, 1975, Phase and amplitude scintillations in the 10 to 40 GHz band, *IEEE Trans. Antennas Propagat., 23*, 792-797.